Applied Physics Letters

Controllable laser output of high-quality cylindrical vector beam through intra-cavity mode conversion

Cite as: Appl. Phys. Lett. **117**, 111105 (2020); https://doi.org/10.1063/5.0020945
Submitted: 06 July 2020 . Accepted: 07 September 2020 . Published Online: 17 September 2020

Yipeng Zhang, Tianxin Wang, Yue Cheng, Dunzhao Wei, Wenzhe Yao, Pengcheng Chen, Yong Zhang, and Min Xiao

AIP Publishing

Applied Physics Letters ARTICLE scitation.org/journal/apl

Controllable laser output of high-quality cylindrical vector beam through intra-cavity mode conversion

Cite as: Appl. Phys. Lett. **117**, 111105 (2020); doi: 10.1063/5.0020945
Submitted: 6 July 2020 · Accepted: 7 September 2020 ·
Published Online: 17 September 2020

Yipeng Zhang,[1] Tianxin Wang,[1] Yue Cheng,[1] Dunzhao Wei,[1,2,a)] Wenzhe Yao,[1] Pengcheng Chen,[1] Yong Zhang,[1,b)] and Min Xiao[1,3]

AFFILIATIONS

[1]National Laboratory of Solid State Microstructures, College of Engineering and Applied Sciences, and School of Physics, Nanjing University, Nanjing 210093, China
[2]School of Physics, Sun Yat-sen University, Guangzhou 510275, China
[3]Department of Physics, University of Arkansas, Fayetteville, Arkansas 72701, USA

[a)]E-mail: weidunzhao@126.com
[b)]Author to whom correspondence should be addressed: zhangyong@nju.edu.cn

ABSTRACT

We experimentally demonstrate the controllable laser output of cylindrical vector (CV) beams, which feature flexibility, high efficiency, and good beam quality. Particularly, the CV laser beams have negligible radial components, distinguishing themselves from the extra-cavity-generated CV beams. The output state is controlled by an intra-cavity vortex half-wave plate (VWP). By changing the topological charge (l) of VWP, we produce $l = 1$ and $l = 2$ CV beams for example. Through rotating the half-wave plate inside the cavity, the laser outputs arbitrary CV beams around the equator of the corresponding high-order Poincaré spheres. For $l = 1$ and $l = 2$ CV beams, the polarization purities are as high as 97.8% and 96.7%, the sloping efficiencies are 15.5% and 5.4%, and the beam quality factors are 2.10 and 3.31, respectively. Our result provides a reliable CV laser source for advanced applications in optical imaging and optical manipulation.

Cylindrical vector (CV) beams[1,2] feature axially symmetric polarizations, which are quite different from the linearly or circularly polarized beams with homogeneous polarization distributions. CV beams have drawn growing attention within the past few decades because of their unique applications based on their transverse and longitudinal field distributions.[3] For example, CV beams have been utilized in stimulated emission depletion (STED) microscopy,[4] edge imaging,[5] and optical trapping.[6] Another striking feature of CV beams is their special focusing properties, which can be used in material processing,[7] high-resolution imaging,[8–12] extraordinary optical transmission,[13] particle manipulation,[14] superfocusing,[15] and optical needles.[16,17] In addition, the orthogonality between CV modes has been recently applied in quantum information processing.[18,19] The rapid developments of practical applications demand CV beams with a good beam quality, high polarization purity, and controllable polarization state.

Generally, one can produce a CV beam by directly passing a linearly polarized Gaussian beam through a spatially anisotropic optical device, such as a q-plate, S-waveplate, vortex half-wave plate (VWP), and so on. These devices have similar working principles, but are fabricated with different materials such as liquid crystal polymers or metasurfaces.[20–23] However, CV beams directly generated by a single spatially anisotropic optical device are accompanied by unwanted radial components, leading to poor beam quality and energy dispersion because of diffraction.[24] Advanced requirements in practical applications demand laser output of CV beams.[25–30] For example, axially birefringent or dichroic materials have been used in a cavity to produce specified CV beams, utilizing their discriminatory loss for e-polarized and o-polarized components.[25–27] Recently, the laser outputs of CV beams were realized by using a Q-plate and metasurface inside the cavity.[28–30] However, it is still a challenge to realize a high-quality and high-efficiency CV beam laser.

In this work, we design a flat-convex-flat cavity with VWP inside to realize a CV beam laser. Due to the intra-cavity polarization conversion through VWP and the mode cleaning effect of the cavity, the directly generated 1064 nm-wavelength CV laser beams show better beam quality than extra-cavity-generated CV beams. By simply altering the VWP, we demonstrate the generation of CV beams carrying topological charges of $l = 1$ and $l = 2$. The measured beam quality factors are 2.10 for $l = 1$ and 3.31 for $l = 2$, respectively, which are close

to the theoretical values. The polarization purities are measured to be 97.8% and 96.7% for $l=1$ and $l=2$ CV beams, respectively. The polarization distribution can be easily controlled by rotating the half-wave plate (HWP) inside the cavity. The sloping efficiencies of $l=1$ and $l=2$ CV beams are 15.5% and 5.4%, respectively.

To avoid the central defect in the commercial VWP, a large cavity mode is required at the VWP position in the cavity to achieve high polarization conversion efficiency and suppress the unwanted modes. Besides, a small cavity mode is required at the location of the laser crystal to match the focused pump beam. Therefore, a flat-convex-flat cavity structure is designed. Figure 1 shows the schematic experimental setup. A continuous-wave 808 nm-wavelength diode laser serves as the pump source. The gain medium is an α-cut 0.5 at. % Nd-doped YVO_4 crystal with a length of 8 mm, which is mounted on a water-cooled copper holder maintained at room temperature and is appropriately oriented to generate horizontally polarized light. The coated front face of the laser crystal serves as the front mirror, which has >99.9% reflectivity at 1064 nm and >97.7% transmittance at 808 nm. The end face has a high antireflection film with >99.8% transmittance at 1064 nm. The laser crystal is placed at the focal position of the pump beam to maximize the energy conversion efficiency. The focused spot size of the pump beam is $\sim$200 μm in diameter. A flat output mirror with 10% transmission at 1064 nm is comprised. A lens with focal length f separates the cavity into two parts. The resonance of the cavity requires that the two lengths L_A and L_B satisfy[31]

$$0 \le \left(1-\frac{L_A}{f}\right)\left(1-\frac{L_B}{f}\right) \le 1. \tag{1}$$

In our experiment, we set $f=200$ mm, $L_A=205$ mm, and $L_B=45$ mm. The selected L_A is slightly larger than f because of the refractive indexes of the intra-cavity optical components. The HWP (Thorlabs Inc.) is set before the lens, while the VWP (Thorlabs Inc.) is placed adjacently behind the lens. Under these parameters, a large cavity mode is designed at the VWP position to fully utilize the effective area of VWP. The cavity mode at the position of the laser crystal is designed to well match the pump beam size. The Jones matrix of the HWP is expressed as

$$M_{HWP}(\beta) = \begin{bmatrix} \cos(2\beta) & \sin(2\beta) \\ \sin(2\beta) & -\cos(2\beta) \end{bmatrix}, \tag{2}$$

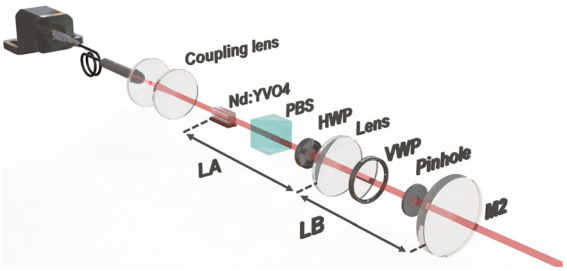

FIG. 1. Sketch of the experimental setup. The experimental setup for generating $l=1$ and $l=2$ CV beams. An Nd:YVO_4 crystal, a convex lens, and an output coupler makeup a flat-convex-flat 1064 nm laser cavity. A polarizing beam splitter (PBS), n HWP, and a VWP are set in sequence. A 1 mm-in-diameter pinhole is close to the output coupler.

where β represents the orientation angle of the HWP. The VWP can be seen as a spatially variant half-wave plate. The orientation of its fast axis is expressed as

$$\alpha(\varphi) = \frac{l}{2}\varphi + \alpha_0, \tag{3}$$

where φ is the azimuthal angle, α_0 refers to the initial orientation angle of its fast axis when $\varphi=0$, and l is a positive integer determined by the VWP. The angular-dependent Jones matrix of the VWP can be written as

$$M_{VWP}(\alpha) = \begin{bmatrix} \cos 2\alpha & \sin 2\alpha \\ \sin 2\alpha & -\cos 2\alpha \end{bmatrix}. \tag{4}$$

When passing a horizontally polarized light, represented by $E_1 = \begin{bmatrix} 1 & 0 \end{bmatrix}^T$ through the HWP and VWP, the output is defined by

$$E_2 = M_{VWP}(\alpha)M_{HWP}(\beta)E_1 = \begin{bmatrix} \cos(l\varphi+2\gamma) \\ \sin(l\varphi+2\gamma) \end{bmatrix}, \tag{5}$$

which shows that the output is the CV beam. Here, $\gamma=\alpha_0-\beta$. In our experiment, the value of α_0 is fixed. The HWP is installed in a rotation stage to control β accurately. By changing l and γ, CV beams with various polarization distributions can be generated. For $l=1$, $\gamma=0$ (or $\pi/4$) corresponds to the output of a typical radially (or azimuthally) polarized beam. In a complete cycle inside the cavity, the light E_1 passes through the HWP and VWP twice, which can be expressed as

$$E_3 = \begin{bmatrix} 1 & 0 \\ 0 & -1 \end{bmatrix} M_{HWP}(-\beta)M_{VWP}(-\alpha) \times \begin{bmatrix} 1 & 0 \\ 0 & -1 \end{bmatrix} M_{VWP}(\alpha)M_{HWP}(\beta)\begin{bmatrix} 1 \\ 0 \end{bmatrix} = E_1. \tag{6}$$

Equation (6) indicates that the cavity design satisfies the self-reproductive condition. Higher-order CV beams can be feasibly produced by using VWPs with higher values of l. In the cavity, a 1 mm-in-diameter pinhole is inserted adjacently to the output mirror to suppress unexpected radial modes. Besides, a PBS is used to remove the unwanted vertically polarized component in front of VWP in the cavity, which is induced by the non-perfect intracavity mode conversion.

First, without putting VWP in the cavity, the laser emits a horizontally polarized Gaussian beam. After passing through HWP and VWP ($\gamma=0$), the Gaussian beam is converted into an extra-cavity-generated CV beam as shown in Figs. 2(b) and 2(e) for $l=1$ and 2, respectively. Here, we use a laser beam profiler (LBP, Newport Corp.) to record the intensity pattern of CV beams. Then, we put the VWP inside the cavity. The laser can directly emit the intra-cavity-generated CV beams as shown in Figs. 2(a) and 2(d) for $l=1$ and 2, respectively. One can observe outer rings (i.e., unwanted components) in the extra-cavity-generated CV beams [Figs. 2(b) and 2(e)]. The higher the value of l is, the more the unwanted components become. In comparison, the intra-cavity-generated CV beams have negligible radial components [Figs. 2(a) and 2(d)]. Figures 2(c) and 2(f) show the 1D intensity profiles across the centers of the generated CV beams. Clearly, in comparison to the extra-cavity-generated CV beams (red dots), the

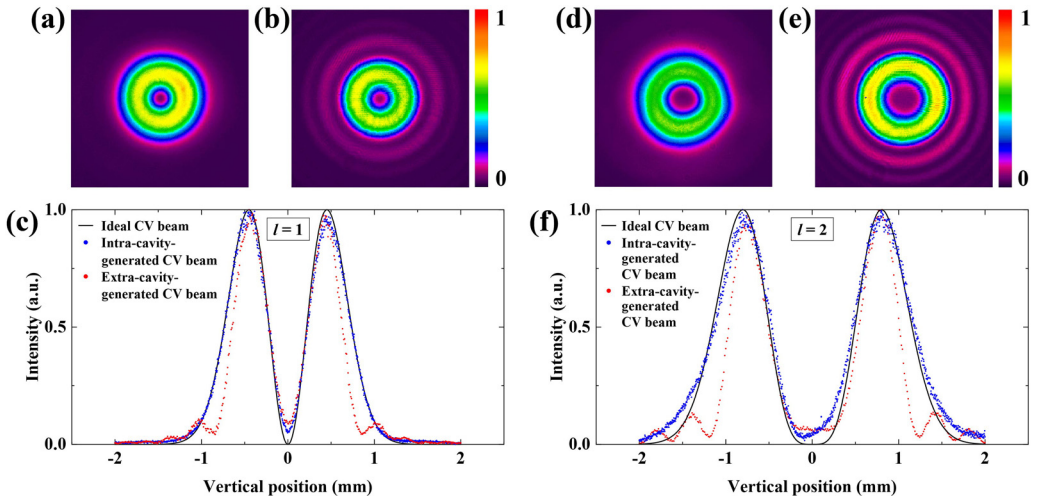

FIG. 2. Intensity patterns of intra (a) and extra-cavity-generated (b) $l=1$ CV beams. Intensity patterns of intra (d) and extra-cavity-generated (e) $l=2$ CV beams. (c) and (f) show the comparisons to an ideal CV beam. Here, $\gamma = 0°$.

intra-cavity-generated CV beams (blue dots) are much closer to the ideal CV beams (black lines).

Arbitrary CV beams around the equator of high-order Poincaré spheres[32] can be obtained by simply changing γ inside the cavity. Figures 3(a)–3(d) and 3(i)–3(l) show the polarization distributions of the output CV beams with $l=1$ and $l=2$, respectively. Here, γ is set to be 0°, 22.5°, 45°, and 67.5°. The white arrows present the polarization distribution of the output CV beams. Then, we use a PBS behind the output coupler to monitor the horizontally polarized components of different CV beams as shown in Figs. 3(e)–3(h) and 3(m)–3(p).

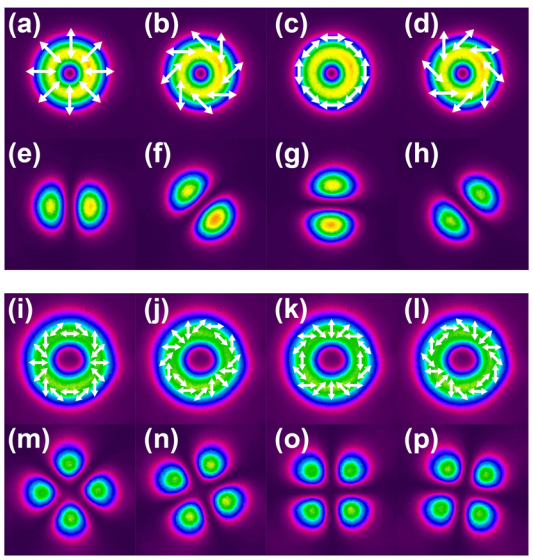

FIG. 3. (a)–(d) and (i)–(l) show the polarization distributions of the intra-cavity-generated $l=1$ and $l=2$ CV beams, respectively, with γ being 0°, 22.5°, 45°, and 67.5°. (e)–(h) and (m)–(p) present the corresponding horizontally-polarized components.

The clear symmetry of the recorded intensity pattern indicates the high polarization purity of the output CV beams.

The polarization purities of the generated CV beams are further analyzed by point-to-point polarization tomography.[20] Here, we select the CV beams in Figs. 3(a) and 3(i) for example. We use a half-wave plate and a PBS to project the polarization of the CV beams into horizontal (H), vertical (V), anti-diagonal (A), and diagonal (D) bases and measure the corresponding intensity I_H, I_V, I_A, and I_D by LBP as shown in Figs. 4(a) and 4(b). To weight the polarization purity of the CV beams, we deduce the Stokes parameters S_1 and S_2 at each pixel of LBP,

$$\begin{cases} S_1 = I_H - I_V, \\ S_2 = I_A - I_D. \end{cases} \tag{7}$$

The azimuthal angle of the polarization ellipse is defined by

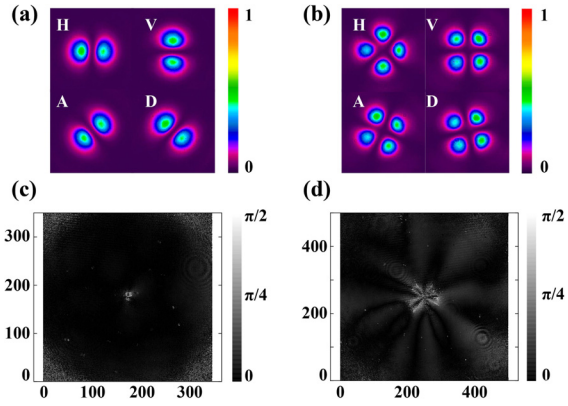

FIG. 4. The measured intensity patterns after CV beams [(a) for $l=1$ and (b) for $l=2$] are projected to horizontal (H), vertical (V), anti-diagonal (A), and diagonal (D) bases. The deviation $\Delta\psi$ from an ideal CV beam ($l=1$ and $l=2$) is shown in (c) and (d).

$$\psi = \frac{1}{2}\arctan\left(\frac{S_2}{S_1}\right). \quad (8)$$

And ψ can be calculated from the experimental data in Figs. 4(a) and 4(b). By comparing the experimental ψ to its theoretical value $\psi_0 = l\varphi$ of an ideal CV beam, we can obtain $\Delta\psi = |\psi_0 - \psi|$, as shown in Fig. 4(c) for $l = 1$ and Fig. 4(d) for $l = 2$. It can be observed that deviation occurs mainly in the central and marginal areas because of the nearly zero intensity. The polarization purities of generated CV beams in Figs. 3(a) and 3(i) are calculated[25] to be 97.8% and 96.7%, respectively.

We also measure the beam quality factors M^2 of the intra-cavity-generated CV beams to be 2.1 and 3.3, which are close to the ideal value of 2 and 3 for $l = 1$ and $l = 2$, respectively. Under pump powers of 1.8 W and 3.4 W, the output powers of $l = 1$ and $l = 2$ CV beams reach 170 mW and 100 mW, respectively. The slope efficiencies of $l = 1$ and $l = 2$ CV beams are measured to be 15.5% and 5.4%, respectively. The insertion losses for $l = 1$ and $l = 2$ VWPs are 4.6% and 18.6%, respectively.

In conclusion, we have demonstrated a compact, high purity, and polarization-controllable CV beam laser. The cavity has been carefully designed to achieve excellent laser performance. In principle, by replacing the VWP, we can produce higher-order CV beams. Besides, our cavity system can be transplanted into other laser and nonlinear systems, such as CV beam pulsed laser and CV beam optical parametric oscillators.

This work was supported by the National Key R&D Program of China (Nos. 2017YFA0303703 and 2016YFA0302500), the National Natural Science Foundation of China (NSFC) (Nos. 91950206 and 11874213), and the Fundamental Research Funds for the Central Universities (No. 14380105).

DATA AVAILABILITY

The data that support the findings of this study are available from the corresponding author upon reasonable request.

REFERENCES

[1]K. S. Youngworth and T. G. Brown, Opt. Express **7**(2), 77 (2000).
[2]D. G. Hall, Opt. Lett. **21**(1), 9 (1996).
[3]Q. W. Zhan, Adv. Opt. Photonics **1**(1), 1 (2009).
[4]S. W. Hell and J. Wichmann, Opt. Lett. **19**(11), 780 (1994).
[5]B. X. Zhang, Z. Z. Chen, H. Sun, J. P. Xia, and J. P. Ding, J. Opt. **18**(3), 035703 (2016).
[6]P. Zhang, Z. Zhang, J. Prakash, S. Huang, D. Hernandez, M. Salazar, D. N. Christodoulides, and Z. Chen, Opt. Lett. **36**(8), 1491 (2011).
[7]C. Hnatovsky, V. Shvedov, W. Krolikowski, and A. Rode, Phys. Rev. Lett. **106**(12), 123901 (2011).
[8]L. Novotny, M. R. Beversluis, K. S. Youngworth, and T. G. Brown, Phys. Rev. Lett. **86**(23), 5251 (2001).
[9]R. Gutbrod, D. Khoptyar, M. Steiner, A. M. Chizhik, A. I. Chizhik, S. Bar, and A. J. Meixner, Nano Lett. **10**(2), 504 (2010).
[10]T. Schmidt, A. I. Chizhik, A. M. Chizhik, K. Potrick, A. J. Meixner, and F. Huisken, Phys. Rev. B **86**(12), 125302 (2012).
[11]G. Bautista, M. J. Huttunen, J. Makitalo, J. M. Kontio, J. Simonen, and M. Kauranen, Nano Lett. **12**(6), 3207 (2012).
[12]X. Xie, Y. Chen, K. Yang, and J. Zhou, Phys. Rev. Lett. **113**(26), 263901 (2014).
[13]P. Banzer, J. Kindler, S. Quabis, U. Peschel, and G. Leuchs, Opt. Express **18**(10), 10896 (2010).
[14]W. Kimura, G. Kim, R. Romea, L. Steinhauer, I. I. Pogorelsky, K. Kusche, R. Fernow, X. Wang, and Y. Liu, Phys. Rev. Lett. **74**(4), 546 (1995).
[15]Z. H. Chen, Y. Zhang, and M. Xiao, J. Opt. Soc. Am. B **32**(8), 1731 (2015).
[16]H. F. Wang, L. P. Shi, B. Lukyanchuk, C. Sheppard, and C. T. Chong, Nat. Photonics **2**(8), 501 (2008).
[17]Y. Z. Zhu, H. J. Wang, Y. H. Zhang, D. M. Liu, W. H. Zhong, Z. D. Gao, G. X. Cui, Y. Q. Lu, Y. Zhang, and M. Xiao, Appl. Phys. Lett. **116**(8), 081106 (2020).
[18]J. T. Barreiro, T. C. Wei, and P. G. Kwiat, Phys. Rev. Lett. **105**(3), 030407 (2010).
[19]A. Sit, F. Bouchard, R. Fickler, J. Gagnon-Bischoff, H. Larocque, K. Heshami, D. Elser, C. Peuntinger, K. Gunthner, B. Heim, C. Marquardt, G. Leuchs, R. W. Boyd, and E. Karimi, Optica **4**(9), 1006 (2017).
[20]F. Cardano, E. Karimi, S. Slussarenko, L. Marrucci, C. de Lisio, and E. Santamato, Appl. Opt. **51**(10), C1 (2012).
[21]D. Lin, J. M. Daniel, M. Gecevicius, M. Beresna, P. G. Kazansky, and W. A. Clarkson, Opt. Lett. **39**(18), 5359 (2014).
[22]S. R. Nersisyan, N. V. Tabiryan, D. Mawet, and E. Serabyn, Opt. Express **21**(7), 8205 (2013).
[23]C. Maurer, A. Jesacher, S. Furhapter, S. Bernet, and M. Ritsch-Marte, New J. Phys. **9**(3), 78 (2007).
[24]B. Sephton, A. Dudley, and A. Forbes, Appl. Opt. **55**(28), 7830 (2016).
[25]G. Machavariani, Y. Lumer, I. Moshe, A. Meir, S. Jackel, and N. Davidson, Appl. Opt. **46**(16), 3304 (2007).
[26]J. F. Bisson, J. Li, K. Ueda, and Y. Senatsky, Opt. Express **14**(8), 3304 (2006).
[27]M. A. Ahmed, A. Voss, M. M. Vogel, and T. Graf, Opt. Lett. **32**(22), 3272 (2007).
[28]H. Kawauchi, Y. Kozawa, S. Sato, T. Sato, and S. Kawakami, Opt. Lett. **33**(4), 399 (2008).
[29]D. Naidoo, F. S. Roux, A. Dudley, I. Litvin, B. Piccirillo, L. Marrucci, and A. Forbes, Nat. Photonics **10**(5), 327 (2016).
[30]H. Sroor, Y. W. Huang, B. Sephton, D. Naidoo, A. Valles, V. Ginis, C. W. Qiu, A. Ambrosio, F. Capasso, and A. Forbes, Nat. Photonics **14**(8), 498 (2020).
[31]V. Magni, Appl. Opt. **25**(1), 107 (1986).
[32]G. Milione, H. I. Sztul, D. A. Nolan, and R. R. Alfano, Phys. Rev. Lett. **107**(5), 053601 (2011).